Synthesis and structural studies of 1-amino-1-deoxy-α-L-*xylo*-hexulopyranose: L-Sorbosamine

Valeri V. Mossine, Todd S. Byrne, Charles L. Barnes & Thomas P. Mawhinney

View supplementary material ⬀

Published online: 19 Mar 2018.

Submit your article to this journal ⬀

Article views: 612

View related articles ⬀

View Crossmark data ⬀

Taylor & Francis
Taylor & Francis Group

SHORT COMMUNICATION

Synthesis and structural studies of 1-amino-1-deoxy-α-L-*xylo*-hexulopyranose: L-Sorbosamine

Valeri V. Mossine[a], Todd S. Byrne[a], Charles L. Barnes[b], and Thomas P. Mawhinney[a]

[a]Department of Biochemistry, University of Missouri, Columbia, Missouri, U.S.A; [b]Department of Chemistry, University of Missouri, Columbia, Missouri, U.S.A.

ABSTRACT

Ketosamines are an important class of glycoconjugates widely employed in clinical diagnostics and implicated in development of diabetic complications, intestinal infections, or advanced cancer, as well as in food organoleptic and nutritional value. We report on the first preparation and structural characterization of 1-amino-1-deoxy-L-sorbose (L-sorbosamine, L-SorNH$_2$). The monosaccharide was synthesized from L-sorbose following a classic phenylosazone protocol. In aqueous solution, L-SorNH$_2$ assumes an anomeric equilibrium consisting of 89.3% α-pyranose, 3.7% β-pyranose, 3.8% α-furanose, 2.4% β-furanose, and 0.9% acyclic *keto* tautomer. The α-pyranose anomer in crystalline L-SorNH$_2 \times$ HCl adopts the $^2C_5$ chair conformation, with bond lengths and valence angles comparing well with related sorbopyranose structures. All hydroxyl oxygen atoms, the ammonium group and chloride ion are involved in an extensive hydrogen bonding network which is formed by infinite chains with fused antidromic $R_7^6(14)$, $R_5^4(10)$, and $R_4^3(8)$ cycles. The Hirshfeld surface analysis suggests a significant contribution of the non-polar intermolecular contacts to the crystal structure, as well.
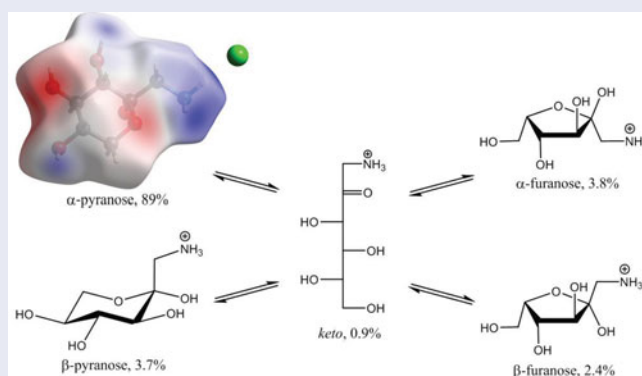
GRAPHICAL ABSTRACT

CONTACT Valeri V. Mossine ✉ MossineV@missouri.edu 🖃 Department of Biochemistry, University of Missouri, Columbia, Missouri, U.S.A

Color versions of one or more of the figures in the article can be found online at www.tandfonline.com/lcar.

🅑 Supplemental data for this article can be accessed on the publisher's website.

Scheme 1. Synthesis of L-sorbosamine from L-sorbose.

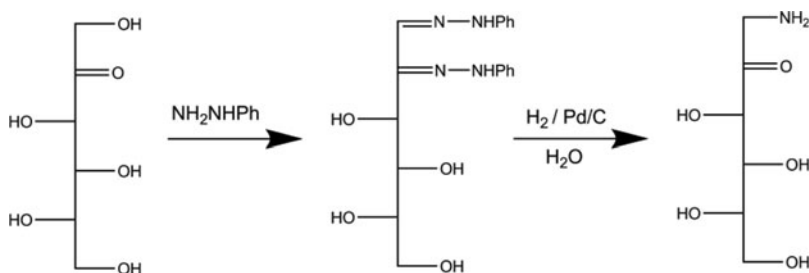Ketosamines is a common name for ketose sugars having one of the hydroxyl groups replaced with an amine. It is a diverse group of glycoaminoconjugates, primarily D-fructosamine derivatives, which are formed both enzymatically and non-enzymatically in biological systems and in food.[1–3] Abundant in organic matter, free glucose, or any other reducing sugar, may interact with free amino groups of amino acids and proteins to form a labile glycosylamine. The latter undergoes the Amadori rearrangement resulting in 1-deoxyketose residue permanently attached to the amine scaffold.[1,4] In this way, reacting glucose ends up as fructosamine derivatives, lactose gives rise to lactulosamines and so on. There is a significant practical interest to ketosamines structure and reactivity due to their omnipresence in living matter. For example, assays for hemoglobin A1c and plasma fructosamine are standard clinical protocols of long-term blood glucose control in diabetes and renal failure,[5,6] while removal of the elevated fructosamine content in proteins may help to control development of diabetic complications.[2] Other examples of potential clinical relevance of fructosamine and other ketosamines include mortality risk from advanced cancer[7,8] and intestinal infections by *Salmonella*.[9] In food sciences, the Maillard reaction is recognized as one of the main sources of chemical changes occurring in foods upon thermal processing and dehydration. It starts with the formation of fructosamine and other 1-deoxy-1-aminoketose derivatives, which undergo further chemical transformations to a large array of both volatile and high-molecular-weight products responsible for characteristic aromas, color and nutritional value of pasteurized, baked, or roasted foods.[1,10]

Structure of D-fructosamine and a number of its derivatives has previously been characterized by NMR and X-ray diffraction in the literature.[11–14] The only known accurately solved structures for other 1-amino-1-deoxy-ketoses are *N*-substituted derivatives of D-tagatose,[15] D-xylulose,[16] and L-rhamnulose.[14] As a part of our program on development of antimetastatic carbohydrate-based agents,[7] we have prepared a previously unknown ketosamine, L-sorbosamine (1-amino-1-deoxy-L-*xylo*-hexulose hydrochloride, L-SorNH$_2$ × HCl), and performed its structural studies by NMR and X-ray diffraction.

L-Sorbosamine was prepared from L-sorbose in two steps (Scheme 1), following a classic phenylosazone protocol.[17] The final synthetic target was purified through recrystallization in ethanol. Its structure was confirmed by both ^{1}H and ^{13}C NMR data.
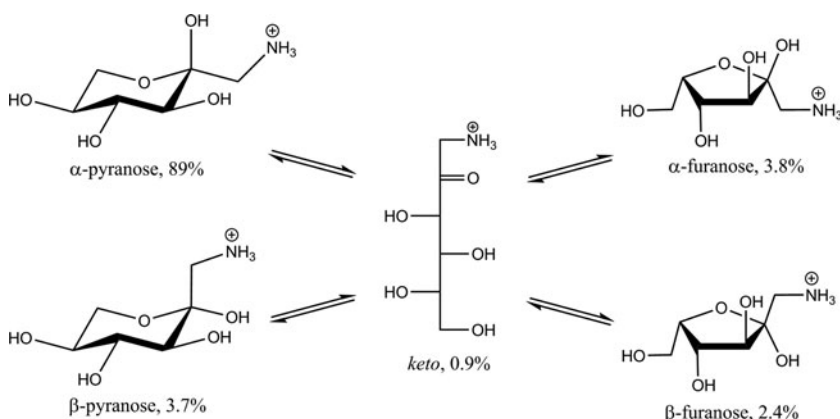
Figure 1. Tautomeric equilibrium in aqueous solution of L-sorbosamine.

According to the NMR data, in neutral aqueous solution L-SorNH$_2$ establishes an equilibrium (Figure 1), with the α-pyranose being a predominant anomeric form and with small, comparable proportions of the α-furanose, β-furanose, and β-pyranose anomers, which do not exceed 4% each (Table 1). There is a notable (0.9%) proportion of the acyclic *keto* tautomer. Previously reported estimates for the population of the acyclic form of L-sorbose in aqueous solutions did not exceed 0.3% (Table 1). On the other hand, an enhanced formation of the acyclic forms was observed in D-fructosamine derivatives with hydrophobic amino substituents that are in close proximity to the carbonyl group and apparently contribute to a significant increase in the acyclic keto tautomer proportion.[12] A similar phenomenon was reported for 1-deoxy-D-sorbose (Table 1), as well.

L-Sorbosamine was obtained in a solid state as a hydrochloride salt. It crystallized exclusively in the α-pyranose form, as evidenced by solid-state ^{13}C NMR data (Figure 2) and the following X-ray diffraction study.

The ORTEP drawing and atomic numbering are shown in Figure 3. The α-L-pyranose ring in crystalline L-SorNH$_2$ × HCl exists in the $^2C_5$ chair conformation, with the Cremer-Pople puckering parameters[22] $Q = 0.5730$ Å, $\theta = 177.02°$, and

Table 1. Tentative assignments of chemical shifts (ppm) in ^{13}C NMR spectra and percentage of L-sorbosamine tautomers in D$_2$O and in solid state at 25°C. For a comparison, the tautomeric compositions for L-sorbose,[18,19] 1-deoxy-D-sorbose,[20,21] and D-fructosamine[11] are given.

| carbon	α-pyranose	β-pyranose	α-furanose	β-furanose	acyclic *keto*	crystalline state
C1	47.88	42.53	45.71	47.74	49.16	47.17
C2	97.77	99.34	102.46	105.66	208.95	95.78
C3	76.33	78.04	85.07	84.07	78.99	73.68
C4	75.49	76.3	80.56	77.26	74.61	72.75
C5	71.92	71.57	81.66	78.70	74.12	69.57
C6	65.03	66.55	63.11	63.79	65.1	63.67
% for L-SorNH$_2$ × HCl	89.3	3.7	3.8	2.4	0.9	100 α-pyr
% for L-Sor	93	2	4	1	0.25	100 α-pyr
% for 1-deoxy-D-Sor	86	8	2.5	<0.8	3.5	100 α-pyr
% for D-FruNH$_2$ × HCl	5	71	11	12	0.8	100 β-pyr
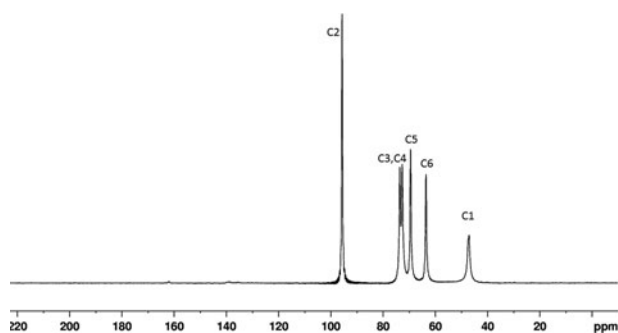
Figure 2. A solid-state ^{13}C NMR spectrum of crystalline L-sorbosamine hydrochloride.

$\phi = 209.86°$. In the ^{1}H NMR spectrum of the major anomer, the vicinal proton-proton coupling constant of H3 and H4, $J_{3,4} = 9.6$ Hz, indicates that they are in the *trans-diaxial* disposition to each other. Hence, the predominant ring conformation of L-sorbosamine in solution must be the $^2C_5$ α-L-sorbopyranose, as well. The related $^2C_5$ conformation of α-L-sorbopyranose[18,23] and $^5C_2$ conformation of 1-deoxy-α-D-sorbopyranose[20,21] were found as the major or the only structure in both solution equilibria and in crystalline state (Table 1). These conformations are enantiomeric and are very close to the sugar ring structure in L-SorNH$_2$ × HCl.

Bond distances and valence angles (Supplementary Tables S4 and S5) in L-sorbosamine compare well to the corresponding values found in α-L-sorbopyranose,[18] 1-deoxy-α-D-sorbopyranose,[21] 1-amino-1-deoxy-β-D-fructopyranose,[11,13,14] and to the average values for a number of crystalline pyranose structures.[24] The endocyclic torsions (Supplementary Table S6) do not differ significantly from the "standard" pyranoside torsions[24] with C–C–C–C(ring) at ~53°, C–C–C–O(ring) – at 55–58°, and C–C–O–C – at ~62°. The exocyclic angles around the ring bonds are close to the "ideal" 60° or 180° as well. The conformation around the C1–C2 bond is *gauche-gauche* and is similar to that found in L-Sor[18] and molecule A in crystalline D-FruNH$_2$ × HCl.[11]

Crystal packing and the intermolecular hydrogen bonds in L-SorNH$_2$ × HCl are shown in Figure 4. The intermolecular H-bonds form a system of infinite chains which are localized in antiparallel layers oriented along the crystallographic *ac* plane. Within the layers, the intermolecular heteroatom contacts are dominated by
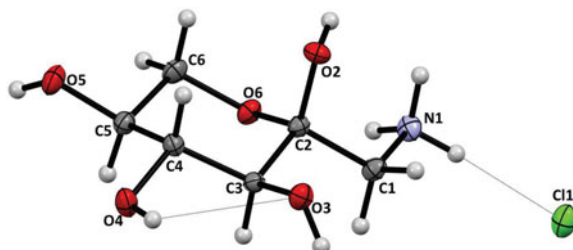

Figure 3. Atomic numbering and displacement ellipsoids at 50% probability level for 1-amino-1-deoxy-L-sorbose hydrochloride. The intramolecular hydrogen bond and the chloride – ammonium contact are shown as dotted lines.
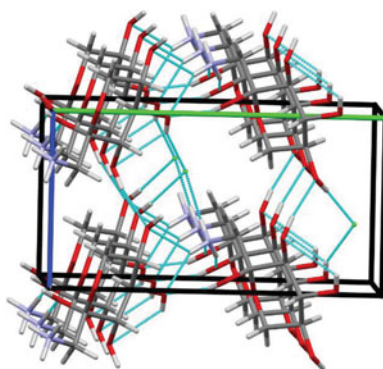
Figure 4. Crystal packing in L-sorbosamine hydrochloride. Hydrogen bonds are shown as cyan dotted lines. Color coding for the crystallographic axes: red – *a*, green – *b*, blue – *c*.

the ammonium group and chloride ions which are involved in 6 out of 8 intermolecular H-bonds (Table 2), serve as centers of multicenter H-bonding and main nodes of the H-bonding network in L-SorNH$_2$ × HCl. A simplified graphical representation of the network is shown in Figure 5. There is a two-dimensional pattern of fused antidromic $R_7^6(14)$, $R_5^4(10)$, and $R_4^3(8)$, rings (according to a topological notation system introduced by Bernstein et al.[25]).

A comparative analysis of the Hirshfeld surfaces[26] calculated for L-sorbosamine (Figure 6) and relative monosaccharides, namely L-sorbose (CCDC 1262281), 1-deoxy-D-sorbose (CCDC 624513), and D-fructosamine (CCDC 715691,715692) was performed in order to get more information in regard with the relative contribution of hydrophilic and hydrophobic intermolecular contacts to the crystal packing forces. The donors and acceptors of strong intermolecular hydrogen bonds are detectable on the Hirshfeld surface as regions of positive and negative electrostatic potential (Figure 6a), reflecting the electrostatic nature of H-bonding. Alternatively, presense of intermolecular contacts can be perceived as regions of increased electron density on the Hirshfeld surface (Figure 6b). The calculations also reveal weak interactions, such as of the C–H···O/Cl type, shown for atoms H3 and H1E in Figure 6c and Table 2.

Table 2. Hydrogen bonding geometry (Å, °) in crystalline L-sorbosamine hydrochloride.

| Contact	D-H	H···A	D···A	D-H···A	Symmetry code
N1-HA···O2	0.91	2.06	2.883(2)	149	x + 1, y, z
N1-HB···Cl1	0.91	2.22	3.125(1)	175	−x + 2, y-1/2, −z + 1
N1-HC···O4	0.91	2.00	2.843(2)	154	−x + 2, y-1/2, −z + 2
N1-HC···O5	0.91	2.58	3.239(2)	130	−x + 2, y-1/2, −z + 2
O2-H···O4	0.79(2)	2.05(2)	2.816(1)	164(2)	−x + 2, y-1/2, −z + 2
O3-H···O5	0.88(3)	2.03(3)	2.878(1)	162(2)	x, y, z-1
O4-H···Cl1	0.75(3)	2.43(3)	3.114(1)	153(3)	x, y, z
O4-H···O3	0.75(3)	2.53(3)	2.885(1)	111(2)	intramolecular
O5-H···Cl1	0.83(3)	2.23(3)	3.058(1)	176(3)	x + 1, y, z + 1
Suspected contacts					
C1-HE···O3	0.99	2.46	3.195(2)	131	x + 1, y, z
C3-H···Cl1	1.00	2.74	3.731(1)	172	x + 1, y, z
C4-H···O6	1.00	2.42	3.363(2)	157	x − 1, y, z
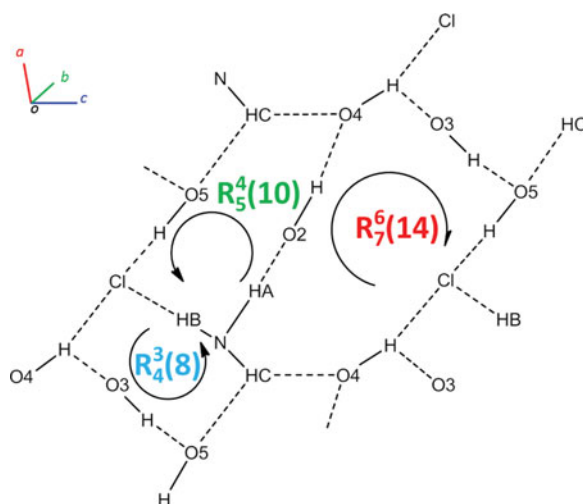
Figure 5. Hydrogen bonding pattern in crystalline L-sorbosamine hydrochloride.

An outlook of intra- and intermolecular atom-to-the-Hirshfeld-surface distances can be integrated in the two-dimensional "fingerprint" plots, such as those calculated for L-sorbosamine and related molecules, as shown in Figure 7. In the plots, each point corresponds to a distinct point on the Heirshfeld surface, with coordinates d_e and d_i corresponding to distances, Å, from the point to a pair of the nearest nuclei exterior and interior to the surface, respectively.[27] The sharp shapes correspond to the closest intermolecular distances such as hydrogen bonds or H···H contacts. One obvious feature displayed by the "fingerprint" plots produced for the sorbopyranose structures is the presence of close H···H contacts that are not as obvious or absent in the fructopyranose structures of D-fructosamine (compare upper and lower rows in Figure 7). This observation suggests a more extensive intermolecular interaction in the α-sorbopyranose structures, as compared to the β-fructopyranoses, and is supported by presence of shorter O···H and Cl···H contacts in the former structures, despite a reverse difference in physical densities of L-SorNH$_2$ × HCl and D-FruNH$_2$ × HCl crystals (calculated as 1.566 and 1.593 g/cm^3, respectively). A more compact crystal packing in D-FruNH$_2$ × HCl may be due to a more extensive density of a three-dimensional intermolecular H-bonding
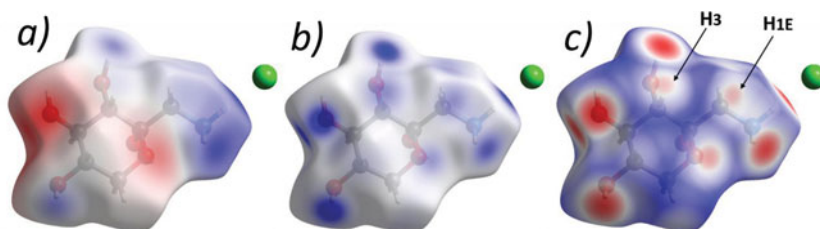

Figure 6. The Hirshfeld surface for L-sorbosamine hydrochloride mapped with: *a)* electrostatic potential in the range −0.136 to +0.204 a.u.; *b)* electron density in the range 0.00 to 0.01 a.u.; *c)* normalized function d_{norm} in the range −0.576 to +1.133 Å. The arrows point at areas of the shortest C-H···O contacts.
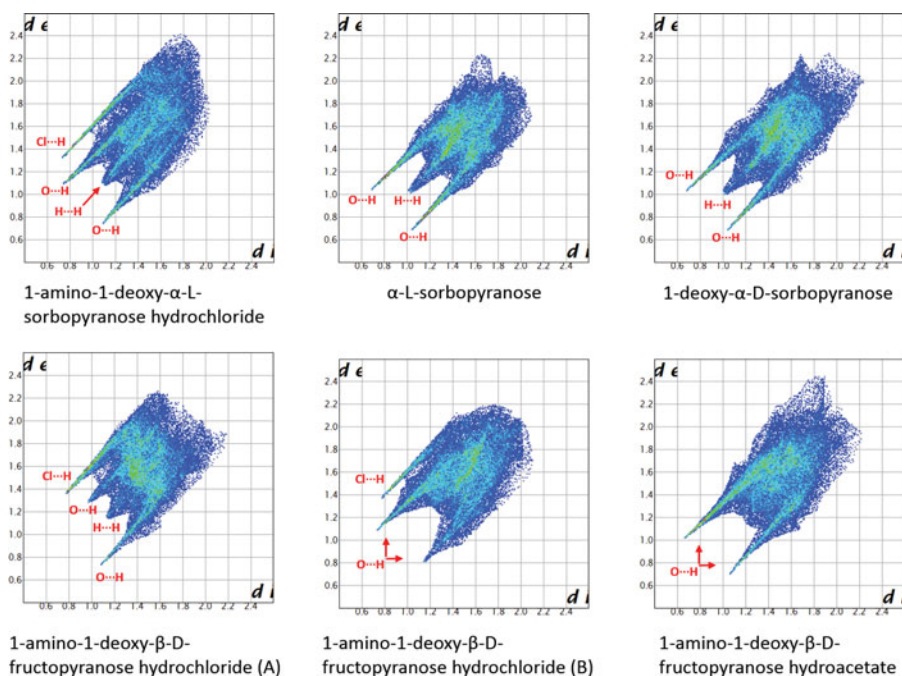
Figure 7. Hirshfeld surface "fingerprint" plots. Labeled sharp features correspond to the types of shortest intermolecular contacts.

network present in the crystal, as compared to the two-dimensional H-bonding net found in L-SorNH$_2$ × HCl (10 H-bonds and 8 H-bonds per molecule, respectively). For a comparison, hydrogen bonding in D-FruNH$_2$ × HOAc is much simpler and is represented by one-dimensional infinite chains, 8 H-bonds per molecule, and the lowest calculated density, at 1.484 g/cm^3. Notably, despite presence of extensive heteroatom contacts in the monosaccharides, the relative contribution of the non-bonding H···H contacts to the crystal packing forces (Table 3) is as significant.

Materials and methods

Synthesis of L-sorbosamine hydrochloride

A solution of 54 g (0.3 mole) of L-sorbose in 1 L of 10% aqueous acetic acid was treated with 108 g (1 mole) of phenylhydrazine at 80 °C for 120 min and the

Table 3. Relative contributions (%) of intermolecular contacts to the Hirshfeld surfaces in crystalline L-SorNH$_2$ × HCl and relevant structures.

Compound	O···H	H···H	H···Cl	Other	Ref
L-SorNH$_2$ × HCl	36.6	49.2	13.5	O···O 0.2; O···Cl 0.6	
L-Sor	45.5	53.4	—	O···O 1.1	[18]
1-deoxy-D-Sor	38.5	61.0	—	O···O 0.4	[21]
D-FruNH$_2$ × HCl (A)	31.9	49.5	18.5	O···O 0.2	[11]
D-FruNH$_2$ × HCl (B)	39.8	50.9	8.3	O···O 0.7; O···Cl 0.2	[11]
D-FruNH$_2$ × HOAc	49.5	49.6	—	C···H 0.8	[11]

product was left to crystallize overnight at 8 °C. The orange precipitate of L-sorbose phenylosazone intermediate was washed with cold water and cold 70% EtOH until essentially free of starting reagents (monitored by TLC). The crystalline mass was dried over $CaCl_2$ *in vacuo* and was used in the subsequent step without further purification.

The crude osazone (20 g) was suspended in a mixture of acetic acid (50 mL), 95% EtOH (100 mL) and H_2O (20 mL). The suspension was hydrogenated in presence of 5 g of 10% palladium on charcoal for 20 h in a hydrogen gas atmosphere at 20–30 psi. When the hydrogenation reaction was essentially complete (proved by TLC), the reaction solution was filtered and repeatedly evaporated/washed with CH_2Cl_2 until free from excessive acetic acid and aromatic amines. The residue was re-dissolved in 200 mL of H_2O and passed through a column charged with Amberlite IRN-78 in Cl^- form. The eluates were decolorized with charcoal, evaporated, and the syrupy residue was mixed with a small volume of ethanol until turbidity. Crystallization at 8 °C for several days yielded 350 mg of L-sorbosamine hydrochloride as colorless prism crystals, which provided monocrystals suitable for the X-ray diffraction studies. ^1H NMR spectrum of the major α-pyranose anomer of L-sorbosamine hydrochloride in D_2O and the resolved coupling constants: δ (ppm) 3.810 (dd, H6B); 3.68 (dd, H6A); 3.64 (m, H5); 3.64 (dd, H4); 3.474 (d, H3); 3.249 (d, H1B); 3.220 (d, H1A); $J_{1A,1B} = -12.8$; $J_{3,4} = 9.6$; $J_{5,6A} = 8.8$; $J_{5,6B} = 5.6$; $J_{6A,6B} = -12$. ^{13}C NMR spectrum of the major α-pyranose anomer of L-sorbosamine hydrochloride in D_2O: δ (ppm) 97.77 (C2); 76.33 (C3); 75.49 (C4); 71.92 (C5); 65.03 (C6); 47.88 (C1). See Table 1 for minor peak assignments in the spectrum and solid-state ^{13}C NMR data.

NMR studies

Solution ^{13}C NMR spectra (D_2O) were recorded at 201.2 MHz and ^1H NMR spectra (D_2O) were obtained at 800.1 MHz using a Bruker AMX800 instrument, with TSPS as an internal standard. The solid-state ^{13}C NMR experiments were done at 75.5 MHz using a Bruker DRX300 wide bore NMR spectrometer equipped with 7 mm solid CP-MAS probe. Zirconia rotors and KEL-F caps were used. The ^{13}C CP-MAS-TOSS spectrum of solid glycine was measured first to check the performance of the spectrometer, and the chemical shift of the carbonyl peak was set to 176.03 ppm. The ^{13}C CP-MAS-TOSS spectrum of the sample was subsequently acquired under the same condition and referenced to this external standard. All samples were measured at room temperature with a spin rate of 5 kHz, 1 msec of contact pulse, and a 4 sec repetition delay.

X-ray diffraction studies

Crystal data and experimental details of the crystallographic studies are given in Supplementary Table 1. The crystal structure was solved with the direct methods program SHELXS-97[28] and refined by full-matrix least squares techniques with the

SHELXL-2017/1[29] suite of programs, with the help of X-Seed.[30] Data were corrected for Lorentz and polarization effects, and for absorption. Non-hydrogen atoms were refined with anisotropic thermal parameters. Hydroxyl and ternary ammonium hydrogen atoms were located in difference Fourier maps and were refined with fixed isotropic thermal parameters. The remaining H-atoms were placed at calculated positions and included in the refinement using a riding model. Crystal structure presentation software: Mercury v. 3.9.[31]

Hirshfeld surface analysis

Generation of wavefunction for calculations of electron density and electrostatic potential were done by the Hartree-Fock method in the STO-3G basis set. The software: CrystalExplorer v. 17.5.[26]

Acknowledgments

References

[1] Mossine, V. V.; Mawhinney, T. P. 1-Amino-1-deoxy-D-fructose ("fructosamine") and its derivatives. *Adv. Carbohydr. Chem. Biochem.* **2010**, *64*, 291–402.

[2] Van Schaftingen, E.; Collard, F.; Wiame, E.; Veiga-da-Cunha, M. Enzymatic repair of Amadori products. *Amino Acids* **2012**, *42*, 1143–1150.

[3] Vladimirov, I. A.; Matveeva, T. V.; Lutova, L. A. Opine biosynthesis and catabolism genes of *Agrobacterium tumefaciens* and *Agrobacterium rhizogenes. Russ. J. Genet.* **2015**, *51*, 121–129.

[4] Yaylayan, V. A.; Huyghues-Despointes, A. Chemistry of Amadori rearrangement products: Analysis, synthesis, kinetics, reactions, and spectroscopic properties. *Crit. Rev. Food Sci. Nutr.* **1994**, *34*, 321–369.

[5] Armbruster, D. A. Fructosamine: Structure, analysis, and clinical usefulness. *Clin. Chem.* **1987**, *33*, 2153–2163.

[6] Shafi, T.; Sozio, S. M.; Plantinga, L. C.; Jaar, B. G.; Kim, E. T.; Parekh, R. S.; Steffes, M. W.; Powe, N. R.; Coresh, J.; Selvin, E. Serum fructosamine and glycated albumin and risk of mortality and clinical outcomes in hemodialysis patients. *Diabetes Care* **2013**, *36*, 1522–1533.

[7] Mossine, V. V.; Glinsky, V. V.; Mawhinney, T. P. Antitumor effects of the early Maillard reaction products. In *The Maillard reaction: Interface between aging, nutrition and metabolism*, Thomas, M. C.; Forbes, J., Eds. Royal Society of Chemistry: **2010**; Vol., pp 170–179.

[8] Malmström, H.; Wändell, P. E.; Holzmann, M. J.; Ärnlöv, J.; Jungner, I.; Hammar, N.; Walldius, G.; Carlsson, A. C. Low fructosamine and mortality – a long term follow-up of 215,011 non-diabetic subjects in the swedish AMORIS study. *Nutr. Metab. Cardiovasc. Dis.* **2016**, *26*, 1120–1128.

[9] Ali, M. M.; Newsom, D. L.; White, P.; Gonzalez, J. F.; Sabag-Daigle, A.; Steidley, B.; Stahl, C.; Dyszel, J. L.; Smith, J. N.; Dieye, Y.; Dubena, J.; Boyaka, P. N.; Krakowka, S.; Arsenescu,

R.; Romeo, T.; Behrman, E. J.; Ahmer, B. M. M. Fructose-asparagine is a primary nutrient during growth of *Salmonella* in the inflamed intestine. *PLoS Pathog.* **2014**, *10*, e1004209.

[10] Finot, P.-A. Historical perspective of the Maillard reaction in food science. *Ann. New York Acad. Sci.* **2005**, *1043*, 1–8.

[11] Mossine, V. V.; Barnes, C. L.; Mawhinney, T. P. Structure of D-fructosamine hydrochloride and D-fructosamine hydroacetate. *J. Carbohydr. Chem.* **2009**, *28*, 245–263.

[12] Mossine, V. V.; Barnes, C. L.; Chance, D. L.; Mawhinney, T. P. Stabilization of the acyclic tautomer in reducing carbohydrates. *Angew. Chem. Int. Ed.* **2009**, *48*, 5517–5520.

[13] Mossine, V. V.; Barnes, C. L.; Mawhinney, T. P. Disordered hydrogen bonding in *N*-(1-deoxy-β-D-fructopyranos-1-yl)-*N*-allylaniline. *Carbohydr. Res.* **2009**, *344*, 948–951.

[14] Mossine, V. V.; Barnes, C. L.; Mawhinney, T. P. The structure of *N*-(1-deoxy-β-D-fructopyranos-1-yl)-L-proline monohydrate ("D-fructose-L-proline") and *N*-(1,6-dideoxy-α-L-fructofuranos-1-yl)-L-proline ("L-rhamnulose-L-proline"). *J. Carbohydr. Chem.* **2007**, *26*, 249–266.

[15] Harding, C. C.; Cowley, A. R.; Watkin, D. J.; Punzo, F.; Hotchkiss, D.; Fleet, G. W. J. 1-Amino-*N,N*-dibenzyl-1-deoxy-α;-D-tagatopyranose methanol solvate. *Acta Cryst.* **2005**, *E61*, o1475–o1477.

[16] Mossine, V. V.; Barnes, C. L.; Feather, M. S.; Mawhinney, T. P. Acyclic tautomers in crystalline carbohydrates: The keto forms of 1-deoxy-1-carboxymethylamino-D-2-pentuloses (pentulose-glycines). *J. Am. Chem. Soc.* **2002**, *124*, 15178–15179.

[17] Maurer, K.; Schiedt, B. A fruitful preparation of glucosamine and a contribution to the catalytic hydrogenation of osazones. *Ber. Dtsch. Chem. Ges.* **1935**, *68B*, 2187–2191.

[18] Nordenson, S.; Takagi, S.; Jeffrey, G. A. α-L-Sorbopyranose: A neutron diffraction refinement. *Acta Cryst.* **1979**, *B35*, 1005–1007.

[19] Angyal, S. J. The composition of reducing sugars in solution. *Adv. Carbohyd. Chem. Biochem.* **1984**, *42*, 15–68.

[20] Jones, N. A.; Jenkinson, S. F.; Soengas, R.; Fanefjord, M.; Wormald, M. R.; Dwek, R. A.; Kiran, G. P.; Devendar, R.; Takata, G.; Morimoto, K.; Izumori, K.; Fleet, G. W. J. Synthesis and NMR studies on the four diastereomeric 1-deoxy-D-ketohexoses. *Tetrahedron Asymm*. **2007**, *18*, 774–786.

[21] Jones, N. A.; Fanefjord, M.; Jenkinson, S. F.; Fleet, G. W. J.; Watkin, D. J. 1-Deoxy-α-D-sorbopyranose. *Acta Cryst.* **2006**, *E62*, o4663–o4665.

[22] Cremer, D.; Pople, J. A. General definition of ring puckering coordinates. *J. Am. Chem. Soc.* **1975**, *97*, 1354–1358.

[23] Symons, M. C. R.; Benbow, J. A.; Pelmore, H. Solvation spectra. Part 74. Interactions between calcium ions and a range of monosaccharides studied by hydroxy-proton resonance spectroscopy. *J. Chem. Soc. Faraday Trans.* **1984**, *1*(80), 1999–2016.

[24] Jeffrey, G. A.; Taylor, R. The application of molecular mechanics to the structures of carbohydrates. *J. Comput. Chem.* **1980**, *1*, 99–109.

[25] Bernstein, J.; Davis, R. E.; Shimoni, L.; Chang, N.-L. Patterns in hydrogen bonding: Functionality and graph set analysis in crystals. *Angew. Chem., Int. Ed. Engl.* **1995**, *34*, 1555–1573.

[26] Spackman, M. A.; Jayatilaka, D. Hirshfeld surface analysis. *CrystEngComm* **2009**, *11*, 19–32.

[27] Spackman, M. A.; McKinnon, J. J. Fingerprinting intermolecular interactions in molecular crystals. *CrystEngComm* **2002**, *4*, 378–392.

[28] Sheldrick, G. M. A short history of SHELX. *Acta Cryst.* **2008**, *A64*, 112–122.

[29] Sheldrick, G. M. Crystal structure refinement with SHELXL. *Acta Cryst.* **2015**, *C71*, 3–8.

[30] Barbour, L. J. X-Seed – a software tool for supramolecular crystallography. *J. Supramol. Chem.* **2003**, *1*, 189–191.

[31] Macrae, C. F.; Bruno, I. J.; Chisholm, J. A.; Edgington, P. R.; McCabe, P.; Pidcock, E.; Rodriguez-Monge, L.; Taylor, R.; van de Streek, J.; Wood, P. A. Mercury CSD 2.0 – new features for the visualization and investigation of crystal structures. *J. Appl. Cryst.* **2008**, *41*, 466–470.